Chemical Engineering Journal 428 (2022) 132444

Contents lists available at ScienceDirect

Chemical Engineering Journal

journal homepage: www.elsevier.com/locate/cej

pH-dependent contribution of chlorine monoxide radicals and byproducts formation during UV/chlorine treatment on clothianidin

Youn-Jun Lee [a], Chang-Gu Lee [a,*], Seong-Jik Park [b], Joon-Kwan Moon [c], Pedro J.J. Alvarez [d]

[a] Department of Environmental and Safety Engineering, Ajou University, Suwon 16499, Republic of Korea
[b] Department of Bioresources and Rural System Engineering, Hankyong National University, Anseong, Republic of Korea
[c] Department of Plant Life and Environmental Sciences, Hankyong National University, Anseong, Republic of Korea
[d] Department of Civil and Environmental Engineering, Rice University, Houston, TX 77005, USA

ARTICLE INFO

Keywords:
Clothianidin
UV/chlorine
Reactive chlorine species
Solution pH
Degradation kinetics

ABSTRACT

Combining UV and free chlorine (UV/chlorine) is an efficient advanced oxidation process for the abatement of recalcitrant organic compounds in drinking water and wastewater. This study investigated the degradation of a neonicotinoid insecticide, clothianidin (CTD), by UV/chlorine treatment. The free chlorine concentration was optimized at 160 μM, and 90.1 ± 0.4% of 40 μM CTD was degraded after 300 s of treatment. Radical quenching tests using *tert*-butyl alcohol, Cl^-, HCO_3^-, and N_3^- indicated that chlorine monoxide (ClO•) was the main radical species for CTD degradation. The second-order rate constants of CTD reacting with ClO• ($k_{ClO•,CTD} = 7.3 \pm 0.1 \times 10^9\ M^{-1}s^{-1}$) was 4.3 times higher than that for •OH ($k_{•OH,CTD} = 1.7 \pm 0.2 \times 10^9\ M^{-1}s^{-1}$). The presence of humic acid inhibited CTD degradation by filtering UV and scavenging ClO•. The pH was optimized at 7, and the overall reaction rate constant (k') was $2.35 \pm 0.02 \times 10^{-2}\ s^{-1}$ (half-life = 0.49 min). Degradation products identified during the UV/chlorine treatment were 1-methyl-3-nitroguanidine ($[M + H]^+ = 118.9$), nitroguanidine ($[M + H]^+ = 105.1$), methylguanidine ($[M + H]^+ = 74.3$), and clothianidin urea ($[M + H]^+ = 206$). The detailed time-dependent concentrations of the generated products under different pH conditions were also provided. The results suggest that the UV/chlorine treatment can be an efficient strategy for CTD degradation.

1. Introduction

Neonicotinoids are a group of systemic insecticides commonly used in the agricultural field for their agonistic effects, which induce paralysis and death in pests [1,2]. The use of neonicotinoids has increased since their launch in the early 1990s, and they represented approximately one-third of the global insecticide market as of 2014 [3]. Clothianidin (CTD) is a neonicotinoid widely used to protect crops from sucking pests [4], but its off-target kills include bees, silkworms, monarch butterflies, and aquatic invertebrates [5–7]. Therefore, CTD overuse can significantly impact the ecological balance. In addition, CTD poses health risks to humans as it inhibits acetylcholine receptors and directly activate the human neuronal-type α4β2 nicotinic receptors (nicotine binding sites in the brain) with strong efficacy [8]. Accordingly, outdoor use of CTD was banned within the European Union in 2018 [1,9]. Despite this restriction, CTD has been detected in aquatic environments in many countries because it is easily transported from agricultural sites to surface and groundwater due to its stability (i.e., its half-life in soils can reach 545 d), high solubility, and non-hydrolysable properties [5,10]. For instance, CTD was detected in a river in Québec, Canada (2–88 ng/L) [11], surface water in Southern Ontario, Canada (maximum concentration of 43.6 ppb) [10], a river in Osaka, Japan (maximum concentration = 12 ng/L) [12], and downstream of a wastewater treatment plant in Iowa, USA (1.7–15.2 ng/L) [13]. In the isotope dilution liquid chromatography tandem mass spectrometry analysis of 13 conventional wastewater treatment plants in the United States, CTD was measured to be 149.7 ± 289.5 ng/L in the influent and 70.2 ± 121.8 ng/L even in the effluent [14]. Furthermore, it was also detected at concentrations as high as 57.3 ng/L in the periodic tap water grab samples from the University of Iowa over 7 weeks in 2016 (May-July) after corn/soybean cultivation [15]. Therefore, appropriate water treatment processes that effectively eliminate such trace levels of CTD are needed.

In this context, advanced oxidation processes (AOPs) are widely used for the oxidation of recalcitrant organic compounds at low concentrations in water. AOPs such as direct UV photolysis [16], UV/H_2O_2 and UV/peroxydisulfate (UV/PDS) [17], photocatalysis [18,19], dielectric

* Corresponding author.
E-mail addresses: changgu@ajou.ac.kr (C.-G. Lee), parkseongjik@hknu.ac.kr (S.-J. Park), jkmoon@hknu.ac.kr (J.-K. Moon), alvarez@rice.edu (P.J.J. Alvarez).

https://doi.org/10.1016/j.cej.2021.132444
Received 4 May 2021; Received in revised form 1 September 2021; Accepted 9 September 2021
Available online 16 September 2021

barrier discharge (DBD) plasma/catalyst [5], and peroxymonosulfate/catalyst [20] have been applied to remove CTD from water. CTD was reported to be moderately degraded by direct photolysis, but radical species such as •OH and $SO_4^{\bullet-}$ generated by the photolysis of H_2O_2 and PDS were not crucial for the CTD degradation [17]. Recently, a treatment combining UV and chlorination (UV/chlorine) has attracted attention as an emerging AOP technology [21–23]. UV and free chlorine ($HOCl/OCl^-$) are widely used for wastewater and drinking water treatment, and their combination can overcome the drawbacks of each process by inactivating pathogenic microorganisms and controlling disinfection by-products (DBPs) [24]. Additionally, because the molar absorption coefficients of HOCl (59 M^{-1} cm^{-1}) and OCl^- (65 M^{-1} cm^{-1}) at a wavelength of 254 nm are 3.3 times higher than that of H_2O_2 [25], the UV/chlorine treatment is an alternative to the UV/H_2O_2 process for the oxidation of recalcitrant organic compounds [25,26]. In particular, the operating cost of UV/chlorine is cheaper than UV, UV/H_2O_2, UV/PDS, and ozonation processes [27,28].

During UV/chlorine treatment, hydroxyl (•OH) and chlorine (Cl•) radicals are produced as primary oxidants by the photolysis of $HOCl/OCl^-$, and they react with $HOCl/OCl^-$ and chloride ions (Cl^-) to generate secondary radicals ($Cl_2^{\bullet-}$, ClO•) (Eqs. (1) to (6)) [29,30].

$$HOCl/OCl^- + h\nu \rightarrow \bullet OH/O^{\bullet-} + Cl\bullet \quad (1)$$

$$Cl\bullet + Cl^- \rightarrow Cl_2^{\bullet-} \left(6.5 \times 10^9 M^{-1}s^{-1}\right) \quad (2)$$

$$\bullet OH + HOCl \rightarrow ClO\bullet \left(2.0 \times 10^9 M^{-1}s^{-1}\right) \quad (3)$$

$$\bullet OH + OCl^- \rightarrow ClO\bullet \left(8.8 \times 10^9 M^{-1}s^{-1}\right) \quad (4)$$

$$Cl\bullet + HOCl \rightarrow H^+ + Cl^- + ClO\bullet \left(3.0 \times 10^9 M^{-1}s^{-1}\right) \quad (5)$$

$$Cl\bullet + OCl^- \rightarrow ClO\bullet + OH^- \left(8.2 \times 10^9 M^{-1}s^{-1}\right) \quad (6)$$

Because the dissociation rate constant (pK_a) of $HOCl/OCl^-$ is 7.5 [31], the speciation of $HOCl/OCl^-$ drastically changes near neutral conditions. The steady-state concentrations of each radical species also change according to the pH conditions [29]. The reactivity of radical species (•OH, Cl•, $Cl_2^{\bullet-}$, ClO•) with each target organic compound depends on their characteristics. For example, •OH generally reacts unselectively with pollutants, and the reaction is close to the diffusion-controlled rate, but reactive chlorine species (RCS) are more selective and more likely to react with compounds containing electron-rich moieties [32]. As the contribution of radicals involved in the reaction varies with different pH conditions, the degradation kinetics and transformation pathways of a pollutant during the UV/chlorine treatment are complex. Moreover, some of the oxidation products generated in UV/chlorine treatment can be much more toxic than the parent pollutant. However, there are no commercial standards for some oxidation products, leading to lack of studies. Therefore, the contribution of radicals under different pH conditions in the UV/chlorine treatment should be investigated along with degradation kinetics and transformation pathways of pollutants.

To the best of our knowledge, this is the first study to investigate the degradation of CTD by a UV/chlorine treatment. The aims of this study are to (1) determine the main reactive radical species responsible for CTD degradation during UV/chlorine treatment; (2) elucidate the effect of pH on the degradation kinetics and contribution of radical species; and (3) identify the transformation pathway of CTD and quantify the concentrations of transformation products that vary with pH conditions in the UV/chlorine treatment.

2. Materials and methods

2.1. Chemical

CTD ($C_6N_5H_8SO_2Cl$, analytical standard), nitrobenzene (NB, $C_6H_5NO_2$, ≥ 99%), 1,4-dimethoxybenzene (DMOB, $C_8H_{10}O_2$ ≥ 99%), atrazine (ATZ, $C_8H_{14}ClN_5$ ≥ 95%), and humic acid (HA, technical grade) were purchased from Sigma-Aldrich Co., Ltd. (St. Louis, MO, USA). Sodium dihydrogen phosphate (NaH_2PO_4, ≥99%), sodium thiosulfate pentahydrate ($Na_2S_2O_3{\cdot}5H_2O$, ≥98.5%), hydrogen peroxide (H_2O_2, 34.5%), sodium chloride (NaCl, ≥99%), *tert*-butyl alcohol (TBA, $C_4H_{10}O$, ≥99%), sodium azide (NaN_3, ≥99%), acetonitrile (ACN, C_2H_3N, high performance liquid chromatography (HPLC) grade, ≥99.9), methyl alcohol (CH_3OH, HPLC grade, ≥99.9%), ethylenediaminetetraacetic acid disodium salt dihydrate ($C_{10}H_{14}Na_2N_2O_8{\cdot}2H_2O$, ≥99.5%), potassium phosphate (KH_2PO_4, ≥99%), and sulfuric acid (H_2SO_4, ≥95%) were purchased from Samchun Pure Chemical Co., Ltd (Pyeongtaek, Korea). Sodium bicarbonate ($NaHCO_3$, ≥99%) and sodium hydrogen phosphate (Na_2HPO_4, ≥98%) were purchased from Daejung Chemicals (Shiheung, Korea). N,N-diethyl-p-phenylenediamine (DPD) sulfate ($C_{10}H_{18}N_2O_4S$) was purchased from Kanto Chemical Co., Inc., (Tokyo, Japan). Sodium hypochlorite (NaClO) was purchased from Junsei Chemical Co., Ltd. (Tokyo, Japan). Potassium permanganate ($KMnO_4$, ≥99.3%) was purchased from Duksan Chemicals (Ansan, Korea). 5,5-Dimethyl-1-pyrroline N-Oxide (DMPO, $C_6H_{11}NO$ ≥ 97%) was purchased from TCI chemicals (Tokyo, Japan). Deionized water (DI) with a resistivity of 18.2 MΩ/cm was obtained from a Direct-Q 3 UV system (Millipore, Massachusetts, USA). All chemicals were used as received.

2.2. Experimental procedure

Free chlorine stock solutions were prepared periodically using sodium hypochlorite, and the respective concentrations were determined using the DPD colorimetric standard method. UV/chlorine experiments were performed in a black acrylic box equipped with a 4 W low-pressure Hg UV-C lamp (TUV G4T5, Philips, USA). The quartz reactor containing 50 mL of the test solution was stirred in the acrylic box, and the solution surface was 6 cm away from the UV-C lamp. The light intensity in the quartz reactor was determined using ferrioxalate actinometry (Text S1) [33]. The calculated photon flux and light intensity were 1.13×10^{-9} Einstein/cm^2/s and 0.53 mW/cm^2. Since the UV light in the reactor was not strictly collimated beam and there may be possible interference from water bath, the optical path length (L) was determined to be 2.76 cm based on the photolysis kinetics of dilute H_2O_2 (Text S2) (Figs. S1 and S2) [34]. Unless otherwise specified, the pH of the test solution was adjusted to 7 using 10 mM sodium phosphate buffer and was measured using a pH meter (Orion Star A211, Thermo, Massachusetts, USA). The scheduled amounts of CTD and free chlorine were spiked into the phosphate buffer solution before UV-C irradiation. At predetermined times, 1 mL of the test solution was sampled, and the residual free chlorine was quenched immediately with 20 μL of 0.05 M sodium thiosulfate. Separately, the concentration of residual free chlorine during CTD degradation by the UV/chlorine treatment was also determined. Sampling was performed at 60 s intervals and the free chlorine concentration was immediately analyzed using a UV–Vis spectrophotometer (NEO-S2117, NEOGEN, Korea) at 515 nm. Photolysis and dark chlorination experiments were conducted without free chlorine and UV-C irradiation, respectively. Degradation experiments were conducted in duplicate (the mean of analytical coefficient of variation, determined as the standard deviation over the mean was 3.76%), and the one tailed *t*-test was used to determine statistically significant differences between treatments at the 95% confidence level ($p < 0.05$).

2.3. Analytical method

CTD and degradation products were analyzed using the Agilent 1100 Series HPLC system (Agilent Technologies Inc., USA) equipped with an autosampler, column compartment, binary pump, solvent degassing unit, and diode array detector. A Phenomenex Luna C18 column (250 mm × 4.6 mm, 5 μm particle size) was used at 25 °C to separate the compounds. The flow rate of the mobile phases consisting of (A) ACN and (B) DI was 1.0 mL/min. From 0 to 2 min, the A/B ratio was set to 15:85, and it linearly changed to 50:50 from 10 to 12 min, and then back to 15:85 from 15 to 20 min. The concentrations of CTD and degradation products (injection volume = 10 μL) were determined based on the peak area corresponding to the retention times. To identify the degradation products, we used a Shimadzu liquid chromatography-tandem mass spectrometry (LC-MSMS) 8040 system (Shimadzu, Japan) with Nexera XR, SIL-20A, LC-20AD, SPD-20A, and CTO-20A. Mobile phases A and B consisted of 0.1% formic acid in DI or ACN, respectively. For the phase separation, a Capcell Core C18 column (OSAKA SODA, Japan) was used at 40 °C. The gradient mobile phase presented the following characteristics: A:B = 90:10 (0–1 min), A:B = 40:60 (15–20 min), A:B = 90:10 (21–25 min), and flow rate of 0.2 mL/min. The total runtime was 20 min, and the injection volume of the sample was 2 μL. The nebulizing gas flow rate was 3 L/min, and the drying flow rate was 15 L/min. Electrospray ionization and positive or negative MS scan modes were used to identify degradation products using collision-induced dissociation gas at 230 kPa and collision energy (CE) of − 25 V for the MS product mode.

The reactive species generated during the UV/chlorine process was identified by an electron spin resonance (ESR) spectrometer (JES-FA200, JEOL, Japan). To obtain stronger radical signals, the concentration of NaOCl in the solution was adjusted to 3.3 mM. DMPO was added to the above solution as a spin trapping agent. Then the UV-C was irradiated to the sample for 10 min. The measurement conditions were as follows: a sweep time of 30 sec, a modulation frequency of 100 kHz, a center field of 336.0 mT, and a microwave frequency of 9.45 GHz.

3. Results and discussion

3.1. Synergistic CTD degradation by UV/chlorine combination

The CTD degradation by UV photolysis, chlorination, and UV/chlorine oxidation with different free chlorine dosages is shown in Fig. 1. After 300 s, the CTD degradation by chlorination alone was negligible (<1%), whereas that by direct UV 254 nm photolysis (159.4 mJ/cm^2) reached 51.1 ± 2.4% with rate constant of 2.4 ± 0.1 × 10^{-3} s^{-1}. The direct photolysis of CTD followed zero-order kinetics (R^2 > 0.99). As water molecules dissociate to hydroxyl radicals when the wavelength of the irradiated UV is less than 190 nm [35], the CTD in our direct photolysis experiment was removed by absorbing photons. The molar absorptivity (ε) of CTD was determined as 15400 M^{-1} cm^{-1} (Fig. S3), which was significantly higher than that of HOCl (101 M^{-1} cm^{-1}) and OCl^- (365 M^{-1} cm^{-1}) [36]. And the quantum yield (Φ_{CTD}) value of the CTD was 0.061 ± 0.002 (Text S3). In contrast, during UV/chlorine treatment, the free chlorine absorbed photons and produced primary radicals (•OH, Cl•), which transformed into secondary radicals (ClO•, $Cl_2^{\bullet-}$) by reacting with HOCl/OCl^- and chloride ions [30]. These generated chloro-radicals enhanced the CTD degradation. When the concentration of free chlorine increased to 0–160 μM, the degradation efficiency rapidly increased. The apparent pseudo-first-order rate constant (k_{app}) for 160 μM free chlorine dosage was 8.1 ± 0.3 × 10^{-3} s^{-1}, which was significantly faster than the k_{app} of direct photolysis (p < 0.05). In addition, 90.1 ± 0.4% of CTD was degraded in 300 s and 160 μM free chlorine was depleted at the same time (Fig. S4). When the initial free chlorine concentration was greater than 160 μM, a fraction of the injected free chlorine remained and k_{app} also increased relatively slowly (Fig. S5). Moreover, k_{app} slightly decreased for chlorine dosages greater than 320 μM (Fig. S6). This result occurred because the contribution of increased secondary radical species (ClO•) was balanced by radical scavenging and the light-screening effect of free chlorine [37]. Chlorine peroxide (Cl_2O_2), an ineffective oxidant, can be produced by recombination of chlorine monoxide radicals (Eq. (7)) [38].

$$ClO\bullet + ClO\bullet \rightarrow Cl_2O_2 \left(k = 2.5 \times 10^9 M^{-1}s^{-1}\right) \quad (7)$$

3.2. Contribution of different radical species

To investigate the role of radical species on the CTD degradation, TBA, Cl^-, HCO_3^-, and azide ion (N_3^-) were added to the UV/chlorine process. TBA can significantly scavenge •OH and Cl• with second-order rate constants of 6.0 × 10^8 and 3.0 × 10^8 $M^{-1}s^{-1}$, respectively [39]. As shown in Fig. 2a, TBA slightly decreased the CTD removal ratio in the UV/chlorine process. At 300 s, 85.7 ± 0.2% CTD was degraded with 1 mM of TBA, which represents an efficiency 4.4% lower than that of the UV/chlorine treatment without TBA. The removal ratios for 10 and 20 mM TBA were 85.3 ± 0.1% and 84.3 ± 0.3%, respectively. There were no significant changes in the CTD degradation for different TBA concentrations. For 20 mM TBA, the results indicate a k_{app} value of 6.3 ± 0.1 × 10^{-3} s^{-1} (Fig. S7), which was 22.2% lower than that of the CTD with no scavenger. Therefore, TBA slightly inhibited the CTD degradation, and other main radical species contributed more significantly to CTD degradation.

Cl^- was added to the samples to further investigate the role of $Cl_2^{\bullet-}$. As Cl^- reacts with •OH and Cl•, it is known to produce Cl• and $Cl_2^{\bullet-}$ as follows [24,37,40].

$$\bullet OH + Cl^- \rightarrow ClOH^{\bullet-} \quad \left(k = 4.3 \times 10^9 M^{-1}s^{-1},\ k_{rev} = 6.1 \times 10^9 M^{-1}s^{-1}\right) \quad (8)$$

$$ClOH^{\bullet-} + H^+ \rightarrow Cl\bullet + H_2O \quad \left(k = 2.1 \times 10^{10} M^{-1}s^{-1}\right) \quad (9)$$

$$Cl\bullet + Cl^- \rightarrow Cl_2^{\bullet-} \left(k = 6.5 \times 10^9 M^{-1}s^{-1}\right) \quad (10)$$

Here, •OH reacts with Cl^- to generate $ClOH^{\bullet-}$ (Eq. (8)). Under acidic conditions, Cl• is generated by the reaction of $ClOH^{\bullet-}$ and H^+ (Eq. (9)), whereas the reverse reaction (Eq. (8)) is promoted under neutral conditions because $ClOH^{\bullet-}$ is not rapidly consumed [24,41]. Therefore, Cl• generation below 10 mM Cl^- is negligible at pH 7 [37,42]. However, $Cl_2^{\bullet-}$ is formed by the consumption of Cl•. Our results show that the CTD removal efficiency remained unchanged after the addition of 10 mM Cl^-. The negligible effect of Cl^- can be explained by the low reactivity of

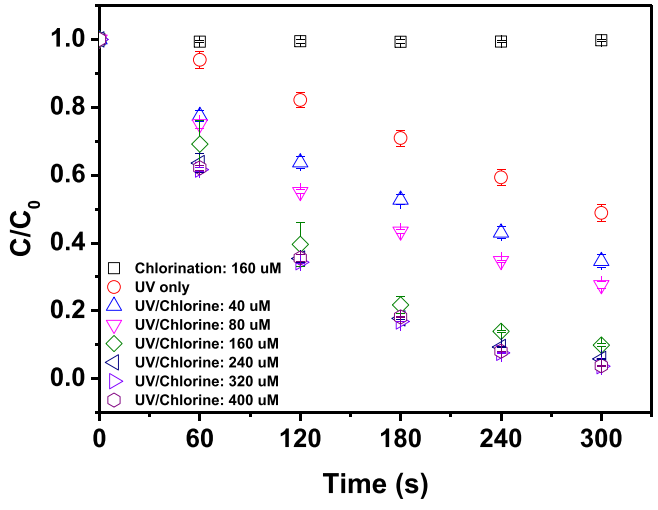

Fig. 1. Degradation kinetics of CTD by UV, chlorination, and UV/chlorine with different free chlorine dosages (pH = 7, $[CTD]_0$ = 40 μM, light intensity = 0.53 mW/cm^2).

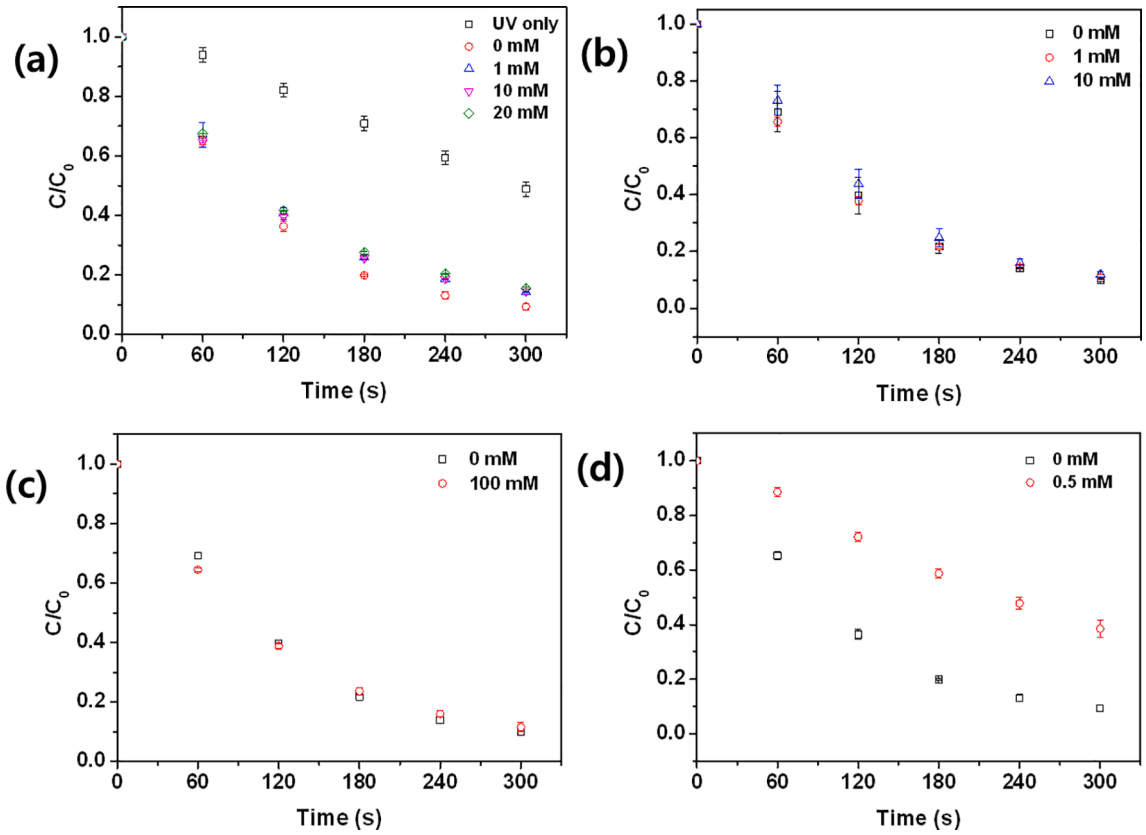

Fig. 2. Effect of (a) TBA, (b) Cl^-, (c) HCO_3^-, and (d) N_3^-on CTD degradation (pH = 7, $[CTD]_0$ = 40 μM, $[free\ chlorine]_0$ = 160 μM, light intensity = 0.53 mW/cm^2).

$Cl_2^{\bullet-}$ and $ClOH^{\bullet-}$ toward CTD.

Next, HCO_3^- and N_3^- were added to the samples to investigate the behavior of ClO• in the CTD degradation by UV/chlorine. HCO_3^- has a low reactivity with ClO• (600 $M^{-1}s^{-1}$), but it rapidly reacts with •OH (8.5 × 10^6 $M^{-1}s^{-1}$), Cl• (2.2 × 10^8 $M^{-1}s^{-1}$), and $Cl_2^{\bullet-}$ (8.0 × 10^7 $M^{-1}s^{-1}$) to form carbonate radical ions ($CO_3^{\bullet-}$) [25,43]. Therefore, ClO• and $CO_3^{\bullet-}$ were available for CTD degradation in the UV/chlorine process with HCO_3^-. However, $CO_3^{\bullet-}$ is a relatively weak oxidant and showed negligible reactivity with CTD (Text S4) (Fig. S8). Therefore, the role of ClO• in the CTD degradation was observed by the addition of HCO_3^-. The results show that the CTD degradation remained unchanged in the presence of 100 mM HCO_3^- (pH = 7.5) (Fig. 2c). On the other hand, N_3^- can significantly scavenge •OH (1.4 × 10^{10} $M^{-1}s^{-1}$), $Cl_2^{\bullet-}$ (5.0 × 10^8 $M^{-1}s^{-1}$), ClO• (2.5 × 10^8 $M^{-1}s^{-1}$), and $CO_3^{\bullet-}$ (1.3 × 10^7 $M^{-1}s^{-1}$) [44], and the CTD degradation was drastically reduced with 0.5 mM N_3^- (Fig. 2d). Since the effects of •OH, $Cl_2^{\bullet-}$, and $CO_3^{\bullet-}$ were not significant and free chlorine was not significantly scavenger with N_3^- (Fig. S9), these results suggest that CTD degradation in the UV/chlorine process is largely attributable to ClO•.

3.3. Reactivity of ClO• and •OH toward CTD

The second-order rate constants of CTD reaction with ClO• ($k_{ClO\bullet,CTD}$) was estimated to evaluate the respective reactivities at pH 8.4 using a reference compound (DMOB), as described in the literature (Text S5) (Fig. S11) [22,26].The second-order rate constant for the reaction of CTD with •OH ($k_{\bullet OH,CTD}$) at a pH range of 5–9 was also determined using ATZ as a reference compound (Text S6) (Figs. S12 and S13). CTD showed a high reactivity with ClO•, presenting a $k_{ClO\bullet,CTD}$ of 7.3 ± 0.1 × 10^9 $M^{-1}s^{-1}$, which is 4.3 times higher the value for •OH ($k_{\bullet OH,CTD}$ = 1.7 ± 0.2 × 10^9 $M^{-1}s^{-1}$). The $k_{ClO\bullet,CTD}$ value was 1–2 orders of magnitude higher than previously reported values for pollutants (e.g., carbamazepine, caffeine, gemfibrozil, bezafibrate, and nalidixic acid), which are primarily degraded by ClO• rather than by other radical species generated in the UV/chlorine treatment [22,26,44]. In addition, the steady-state concentration of ClO• was 3 to 4 orders of magnitude higher than those of •OH and Cl• in the UV/chlorine process [26,30,45]. Accordingly, the high reactivity of CTD with ClO• and the relatively higher steady-state concentration of ClO• than those of •OH and Cl• confirmed the importance of ClO• for the CTD degradation during UV/chlorine treatment.

3.4. Effect of natural organic matter (NOM)

The presence of NOM in aquatic environments is common. NOM hinders the performance of UV/chlorine AOP by filtering UV and scavenging RCS, especially ClO• [21,22,26]. HA was used to evaluate the effect of NOM on the UV/chlorine process. The CTD removal efficiency in the UV/chlorine process at 300 s with 0, 0.23, 1.15, and 2.30 mg C/L of HA were 90.4 ± 0.4%, 85.3 ± 0.5%, 81.0 ± 0.3%, and 76.0 ± 3.0%, respectively (Fig. 3a). As the HA concentration increased from 0 to 2.30 mg C/L, the k_{app} of CTD significantly decreased from 8.2 ± 0.5 × 10^{-3} to 4.9 ± 0.5 × 10^{-3} s^{-1}. The measured molar absorption coefficient of HA was 0.078 $(mg\ C/L)^{-1}cm^{-1}$ (Fig. S14), which suggests that the number of photons absorbed by CTD and the radicals generated by the free chlorine decreased by the addition of HA. Moreover, NOM can compete with CTD to react with •OH, Cl•, and ClO• with second-order rate constants of 2.5 × 10^4, 1.3 × 10^4, and 4.5 × 10^4 $(mg/L)^{-1}s^{-1}$, respectively [44]. As ClO• was crucial for the CTD degradation by the UV/chlorine treatment, the scavenging of ClO• by HA significantly decreased the CTD degradation efficiency. Similar results were also found in the actual water test using secondary effluent (Fig. S15), and k_{app} of CTD in secondary wastewater was 3.7 ± 0.1 × 10^{-3} s^{-1}.

ESR spectra were obtained to identify the predominant free radicals (Fig. 3b). A typical seven-fold spectrum with an intensity ratio of 1:2:1:2:1:2:1 was observed in the UV/chlorine treatment, which

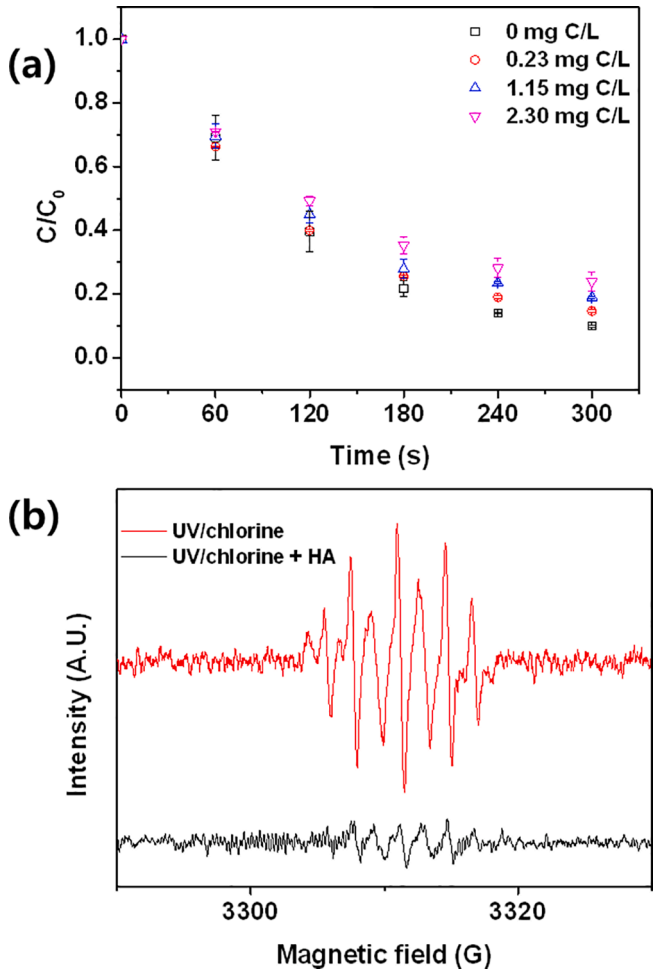

Fig. 3. (a) Effect of HA on degradation of CTD and (b) ESR spectra of UV/chlorine process in the absence and presence of HA (degradation experiment condition: pH = 7, $[CTD]_0$ = 40 μM, $[\text{free chlorine}]_0$ = 160 μM, light intensity = 0.53 mW/cm^2, ESR experiment condition: pH = 7, $[\text{free chlorine}]_0$ = 3.3 mM, light intensity = 0.53 mW/cm^2, HA = 2.30 mg C/L).

indicates the oxidation of DMPO to 5-*tert*-butoxycarbonyl-methyl-2-oxo-pyrroline-1-oxyl (DMPOX) by the various oxidizing substances [46]. Based on previous studies, this DMPOX spectrum can be attributed to the RCS and •OH in the UV/chlorine treatment [47,48]. From the above scavenging test results, it can be concluded that ClO• drives this oxidation. When HA was added during the UV/chlorine treatment, the detection of DMPOX signal was significantly decreased. This result is in line with CTD degradation experiment in the presence of HA, and it corroborates that HA reacts with ClO• and inhibits CTD degradation.

3.5. Effect of pH on the kinetics of reactive species

To identify the contribution of each reactive species to the CTD degradation in the UV/chlorine treatment ($[CTD]_0$ = 5 μM, $[\text{free chlorine}]_0$ = 160 μM, light intensity = 0.53 mW/cm^2), the rate constants of direct UV photolysis, •OH, and RCS were quantified using radical probes. The steady-state concentrations of •OH ($[•OH]_{ss}$) in the UV/chlorine process with different pH values were determined using NB as an •OH probe (Text S7) (Fig. S16). The pseudo-first-order rate constants of the CTD degradation by UV (k_{uv}), •OH ($k_{•OH}$), and RCS (k_{RCS}) were determined using the obtained $[•OH]_{ss}$ and $k_{ClO•,CTD}$, as detailed in Text S8. The overall reaction rate constants (k'), k_{uv}, $k_{•OH}$, and k_{RCS} at different pH values are shown in Fig. 4. Whereas changes in k_{uv} were negligible, $k_{•OH}$ was greatly affected by pH under acidic conditions. The

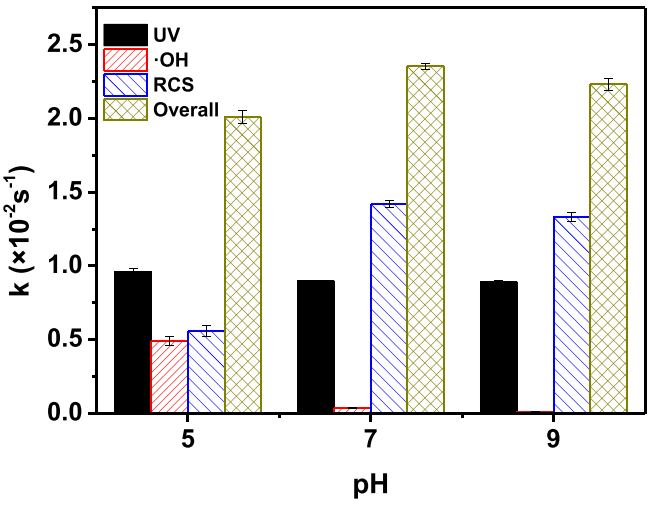

Fig. 4. Rate constants of radical species of CTD degradation under different pH by UV/chlorine treatment ($[NB]_0$ = 5 μM, $[CTD]_0$ = 5 μM, $[\text{free chlorine}]_0$ = 160 μM, light intensity = 0.53 mW/cm^2).

fraction of $k_{•OH}$ for CTD degradation at pH 5, 7, and 9 were 24.4%, 1.5%, and 0.5%, respectively. This result could be explained by the effect of pH on the dissociation of HOCl/OCl$^-$. As the pK_a of HOCl/OCl$^-$ was 7.5, the speciation of OCl$^-$ increased as the pH increased from 5 to 9 [49]. The quantum yields of HOCl (0.62) and OCl$^-$ (0.55) were not significantly different, but the formation of ClO• by the reaction of OCl$^-$ with •OH or Cl• was 4.4 and 2.7 times faster than that with HOCl, respectively [50]. Therefore, the generation of ClO• was promoted with increasing pH, but the production of $[•OH]_{ss}$ decreased. The calculated $[•OH]_{ss}$ at pH 5 was 12.5 and 37.8 times higher than the values at pH 7 and 9 (Text S7), which is consistent with the result of the •OH probe (NB) degradation test in the UV/chlorine process (Fig. S17). As $k_{ClO•,CTD}$ did not change with pH (Fig. S18) ($k_{ClO•,CTD} = 1.7 \pm 0.2 \times 10^9$ M^{-1}s^{-1}), the relatively high contribution of •OH to CTD degradation at pH 5 was attributed to the higher production of $[•OH]_{ss}$. Accordingly, the k' values at pH 5, 7, and 9 were $2.01 \pm 0.05 \times 10^{-2}$, $2.35 \pm 0.02 \times 10^{-2}$, and $2.23 \pm 0.04 \times 10^{-2}$ s^{-1}, respectively. Therefore, the k' value was the highest at pH 7 (half-life = 0.49 min). At pH 5, the lack of ClO• contribution (k_{RCS}) under acidic conditions was replenished by the contribution of •OH ($k_{•OH}$), but it was not completely compensated. When the pH increased to 9, the concentration of OH$^-$ in the solution also increased, which rapidly scavenged ClO• with a reaction rate constant of 2.5×10^9 M^{-1}s^{-1} [23].

3.6. Transformation products of CTD

Transformation intermediates during the UV/chlorine treatment were identified using HPLC and LC-MSMS with a full scan spectrum and product ion scan in positive or negative mode (Fig. S19). Fig. 5 shows the proposed degradation pathway of CTD during the UV/chlorine treatment. The molecular weights and product ions of identified compounds are summarized in Table S1. The CTD $[M + H]^+$ peak at 250 m/z corresponded to a retention time of 7.106 min, and the product ions were obtained for m/z = 169, 168.1, and 85.1. The daughter with m/z = 169 was obtained by the loss of Cl and NO_2 from the CTD [16,51]. The evolution of $[M + H]^+$ m/z = 118.9 at 2.556 min was confirmed by the 1-methyl-3-nitroguanidine obtained from the product ions of m/z = 73.2, 44.2, and 43.2. In addition, 1-methyl-3-nitroguanidine was formed during the initial stage of CTD degradation by the dissociation of the C-N linkage. The 1-methyl-3-nitroguanidine further transformed to nitroguanidine (m/z = 105.1) and methylguanidine (m/z = 74.3) by N-demethylation and reduction of the nitro group, respectively. The $[M + H]^+$clothianidin urea (m/z = 206) was another identified transformation

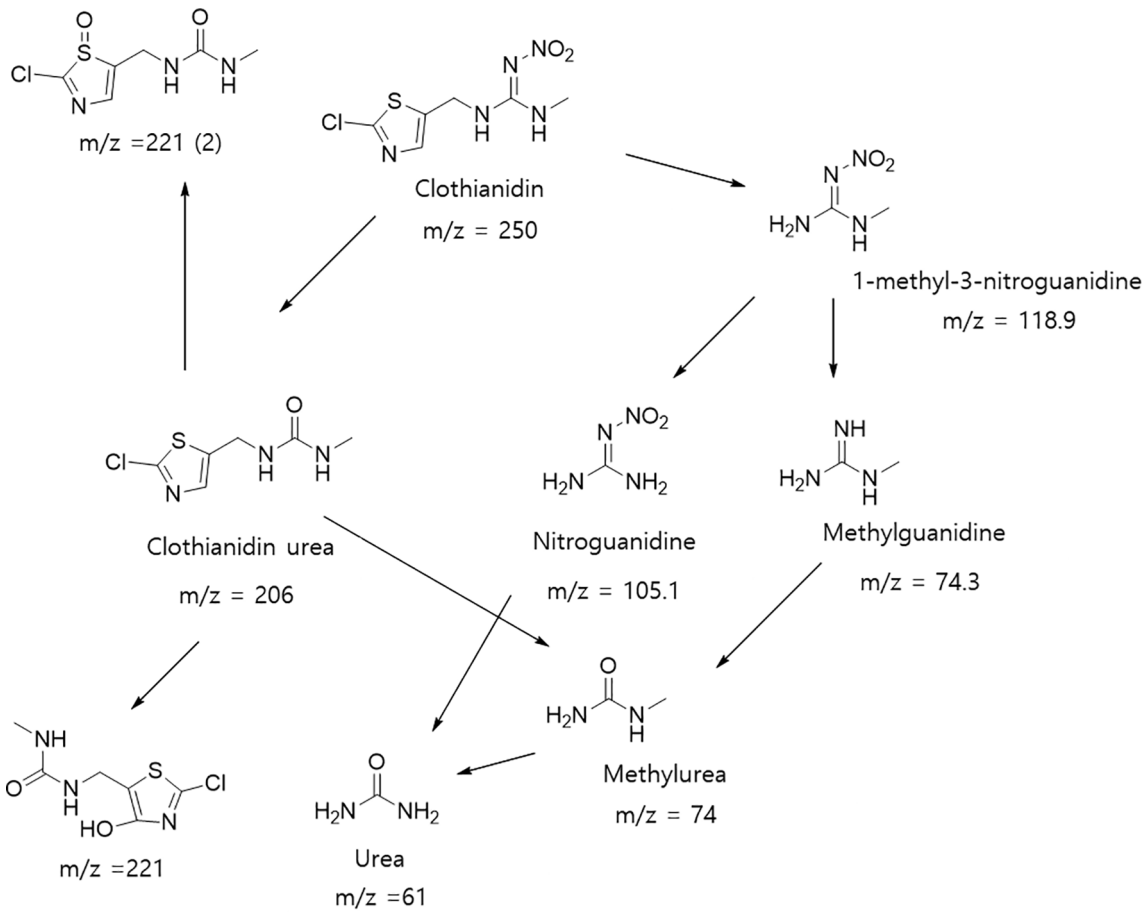

Fig. 5. Proposed degradation pathway of CTD during the UV/chlorine treatment (pH = 7, $[CTD]_0$ = 40 μM, $[free\ chlorine]_0$ = 160 μM, light intensity = 0.53 mW/cm^2.)

product at the initial stage of CTD degradation. Its mass spectrum for retention time of 6.761 min was confirmed by major fragments of m/z = 132.1, 86.1, 170.5. As the methyl group at the end of the chain structure was easily detached [5], ClO• and UV could attack the C- atom of C = N moieties of CTD to substitute the nitroimino moiety of the urea compound, which was similar to those of UV, $•O_2^-$, and •OH in previous studies [5,19]. After transformation, the thiazole ring of CTD urea was hydroxylated by ClO• to form m/z = 221. As reported by Kong et al. [22], ClO• can induce hydroxylation in the UV/chlorine treatment. In a different pathway, the thiazole ring of CTD urea was likely converted to thiazole 1-oxide to form m/z = 221 (2).

To compare the detailed evolution profile during the UV/chlorine process under different pH conditions and UV photolysis without free chlorine (UV only), the time-dependent concentration of the main degradation products (1-methyl-3-nitroguanidine, clothianidin urea, and methyl guanidine) at each sampling time was quantified (Fig. 6). Fig. 6a shows the evolution of 1-methyl-3-nitroguanidine over 300 s. When the pH was 7, its concentration of was the highest (0.40 mg/L) at 180 s, and it decreased to 0.25 mg/L at 300 s. At pH 5 and 9, the concentration increased from 0 mg/L (0 s) to 0.17 and 0.12 mg/L (120 s), respectively, and there was no significant concentration difference after 120 s. Compared to the treatment with UV only, the chlorine addition drastically improved the evolution of 1-methyl-3-nitroguanidine, which indicates that the transformation of CTD to 1-methyl-3-nitroguanidine due to the dissociation of C-N linkage was promoted by radical species, probably •OH (pH 5) and ClO• (pH 5, 7, and 9). The transformation of CTD to 1-methyl-3-nitroguanidine by •OH and breaking of the C-N bond connects the nitroguanidine and thiazole ring by electrocatalysis, as reported in previous studies [19,52]. After CTD was transformed to 1-methyl-3-nitroguanidine at the initial stage of CTD degradation, 1-methyl-3-nitroguanidine was further decomposed and methylguanidine was formed (Fig. 6b). The graph of methylguanidine evolution shows an upward trend under all reaction conditions. As 1-methyl-3-nitroguanidine was more effectively generated in the presence of free chlorine, the concentration of methylguanidine at pH 5, 7, and 9 was higher for the combined treatment than for UV only. Therefore, the transformation pathway of CTD to 1-methyl-3-nitroguanidine was mostly related to radical species rather than photons. Fig. 6c shows the evolution of clothianidin urea. The evolution characteristics of clothianidin urea were different from those of 1-methyl-3-nitroguanidine and methylguanidine. The generation of clothianidin urea for the treatment with only UV was superior at pH 5 than at pH 7 and 9. This observation implies that CTD was more efficiently transformed to clothianidin urea by photons than by radical species. Additionally, clothianidin urea was likely more efficiently oxidized by ClO• than by •OH and photons because its abundance was inversely proportional to the contribution of ClO• (pH 7 and 9).

ECOSAR is a quantitative structure activity relationship (QSAR) based program that is widely used for the estimation of compound toxicity in water treatment [39,53]. Transformation byproducts may possess a potential risk for aquatic organisms and human health. Thus, the potential toxicity of byproducts was theoretically estimated (Table S2). Among the predominant first-stage product, 1-methyl-3-nitroguanidine and methylguanidine, which results from attack by radical species, presented lower acute and chronic toxicity than CTD, but clothianidin urea, which results from UV photolysis, presented higher acute toxicity for green algae and higher chronic toxicity for fish and green algae. Based on this theoretical toxicity estimation, treatment

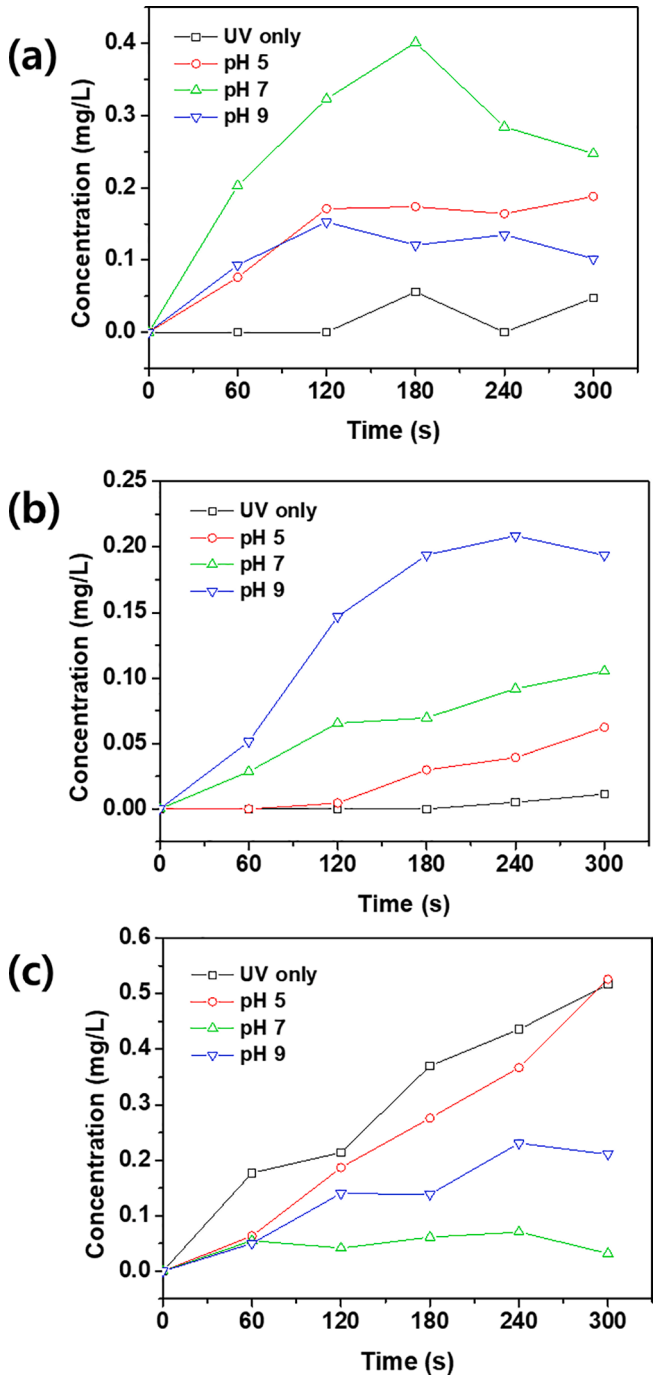

Fig. 6. Changes in the concentration of (a) 1-methyl-3-nitroguanidine, (b) methylguanidine, and (c) clothianidin urea with different pH conditions during the degradation of CTD by the UV/chlorine treatment ($[CTD]_0 = 40$ μM, $[\text{free chlorine}]_0 = 160$ μM, light intensity = 0.53 mW/cm^2).

by the generated radicals should participate in the CTD oxidation to decrease the overall toxicity. However, the evolution of degradation products can vary with water matrix and background organics, so further study is needed to verify detoxification under other experimental conditions.

4. Conclusions

This study advances understanding of CTD degradation by the UV/chlorine treatment (and the importance of pH optimization) for the purification of drinking water and wastewater. CTD was efficiently degraded by photons and ClO• generated during the UV/chlorine treatment. Scavenger tests to distinguish the radicals contribution indicated that CTD was primarily degraded by ClO•, and the estimated $k_{ClO\bullet,CTD}$ ($7.3 \pm 0.1 \times 10^9$ M^{-1}s^{-1}) indicated the high reactivity of CTD with ClO•. In addition, NOM interfered with the UV/chlorine performance by filtering the UV and scavenging the RCS. Furthermore, k_{uv} showed negligible changes under different pH conditions, whereas pH greatly affected $k_{\bullet OH}$ under acidic conditions. The generation of ClO• was promoted by increasing pH, but the overall reaction rate constant (k') was optimized at pH 7. The two main byproducts were of 1-methyl-3-nitroguanidine (formed primarily by radicals attack) and clothianidin urea (formed primarily by photolysis), and quantitative structure activity relationships using ECOSAR inferred that the radical attack results in less toxic byproducts. Overall, these encouraging results suggest that the UV/chlorine treatment should be considered as an effective alternative to degrade CTD and possibly other recalcitrant organic compounds.

Declaration of Competing Interest

The authors declare that they have no known competing financial interests or personal relationships that could have appeared to influence the work reported in this paper.

Acknowledgements

This work was supported by Korea Environment Industry & Technology Institute(KEITI) through the project to develop eco-friendly new materials and processing technology derived from wildlife, funded by the Ministry of Environment of Korea (2021003240003), and partial funding for PJA was provided by the NSF ERC for Nanotechnology-Enabled Water Treatment (EEC-1449500).

Appendix A. Supplementary data

Supplementary data to this article can be found online at https://doi.org/10.1016/j.cej.2021.132444.

References

[1] R.J. Lennon, R.F. Shore, M.G. Pereira, W.J. Peach, J.C. Dunn, K.E. Arnold, C. D. Brown, High prevalence of the neonicotinoid clothianidin in liver and plasma samples collected from gamebirds during autumn sowing, Sci. Total Environ. 742 (2020), 140493.
[2] S. Ohno, Y. Ikenaka, K. Onaru, S. Kubo, N. Sakata, T. Hirano, Y. Mantani, T. Yokoyama, K. Takahashi, K. Kato, K. Arizono, T. Ichise, S.M.M. Nakayama, M. Ishizuka, N. Hoshi, Quantitative elucidation of maternal-to-fetal transfer of neonicotinoid pesticide clothianidin and its metabolites in mice, Toxicol. Lett. 322 (2020) 32–38.
[3] R.J. Lennon, W.J. Peach, J.C. Dunn, R.F. Shore, M.G. Pereira, D. Sleep, S. Dodd, C. J. Wheatley, K.E. Arnold, C.D. Brown, From seeds to plasma: confirmed exposure of multiple farmland bird species to clothianidin during sowing of winter cereals, Sci. Total Environ. 723 (2020), 138056.
[4] B. Atta, M. Rizwan, A.M. Sabir, M.D. Gogi, M.A. Farooq, A. Jamal, Lethal and sublethal effects of clothianidin, imidacloprid and sulfoxaflor on the wheat aphid, Schizaphis graminum (Hemiptera: Aphididae) and its coccinellid predator, Coccinella septempunctata, Int. J. Trop. Insect Sci. 41 (1) (2021) 345–358.
[5] S. Li, H. Chen, X. Wang, X. Dong, Y. Huang, D. Guo, Catalytic degradation of clothianidin with graphene/TiO2 using a dielectric barrier discharge (DBD) plasma system, Environ. Sci. Pollut. Res. 27 (23) (2020) 29599–29611.
[6] J.C. Miles, J. Hua, M.S. Sepulveda, C.H. Krupke, J.T. Hoverman, Effects of clothianidin on aquatic communities: evaluating the impacts of lethal and sublethal exposure to neonicotinoids, PLoS One 12 (2017), e0174171.
[7] J.R. Pecenka, J.G. Lundgren, Non-target effects of clothianidin on monarch butterflies, Naturwissenschaften 102 (2015) 19.
[8] P. Li, J. Ann, G. Akk, Activation and modulation of human alpha4beta2 nicotinic acetylcholine receptors by the neonicotinoids clothianidin and imidacloprid, J. Neurosci. Res. 89 (2011) 1295–1301.
[9] C. Zhang, F. Li, R. Wen, H. Zhang, P. Elumalai, Q. Zheng, H. Chen, Y. Yang, M. Huang, G. Ying, Heterogeneous electro-Fenton using three-dimension NZVI-BC electrodes for degradation of neonicotinoid wastewater, Water Res. 182 (2020), 115975.

[10] K. Basley, D. Goulson, Neonicotinoids thiamethoxam and clothianidin adversely affect the colonisation of invertebrate populations in aquatic microcosms, Environ. Sci. Pollut. Res. 25 (10) (2018) 9593–9599.
[11] J.M. Montiel-León, S.V. Duy, G. Munoz, M. Amyot, S. Sauvé, Evaluation of on-line concentration coupled to liquid chromatography tandem mass spectrometry for the quantification of neonicotinoids and fipronil in surface water and tap water, Anal. Bioanal. Chem. 410 (11) (2018) 2765–2779.
[12] A. Yamamoto, T. Terao, H. Hisatomi, H. Kawasaki, R. Arakawa, Evaluation of river pollution of neonicotinoids in Osaka City (Japan) by LC/MS with dopant-assisted photoionisation, J. Environ. Monit. 14 (8) (2012) 2189, https://doi.org/10.1039/c2em30296a.
[13] M.L. Hladik, D.W. Kolpin, First national-scale reconnaissance of neonicotinoid insecticides in streams across the USA, Environ. Chem. 13 (1) (2016) 12, https://doi.org/10.1071/EN15061.
[14] A.M. Sadaria, S.D. Supowit, R.U. Halden, Mass balance assessment for six neonicotinoid insecticides during conventional wastewater and wetland treatment: nationwide reconnaissance in United States wastewater, Environ. Sci. Technol. 50 (2016) 6199–6206.
[15] K.L. Klarich, N.C. Pflug, E.M. DeWald, M.L. Hladik, D.W. Kolpin, D.M. Cwiertny, G. H. LeFevre, Occurrence of neonicotinoid insecticides in finished drinking water and fate during drinking water treatment, Environ. Sci. Technol. Lett. 4 (5) (2017) 168–173.
[16] Y. Gong, J. Chen, H. Wang, J. Li, Separation and identification of photolysis products of clothianidin by ultra-performance liquid tandem mass spectrometry, Anal. Lett. 45 (17) (2012) 2483–2492.
[17] J.L. Acero, F.J. Real, F. Javier Benitez, E. Matamoros, Degradation of neonicotinoids by UV irradiation: kinetics and effect of real water constituents, Sep. Purif. Technol. 211 (2019) 218–226.
[18] Y.-J. Lee, J.-K. Kang, S.-J. Park, C.-G. Lee, J.-K. Moon, P.J.J. Alvarez, Photocatalytic degradation of neonicotinoid insecticides using sulfate-doped Ag3PO4 with enhanced visible light activity, Chem. Eng. J. 402 (2020), 126183.
[19] D. Mohanta, M. Ahmaruzzaman, A novel Au-SnO2-rGO ternary nanoheterojunction catalyst for UV-LED induced photocatalytic degradation of clothianidin: identification of reactive intermediates, degradation pathway and in-depth mechanistic insight, J. Hazard. Mater. 397 (2020), 122685.
[20] P. Duan, Y. Qi, S. Feng, X. Peng, W. Wang, Y. Yue, Y. Shang, Y. Li, B. Gao, X. Xu, Enhanced degradation of clothianidin in peroxymonosulfate/catalyst system via core-shell FeMn @ N-C and phosphate surrounding, Appl. Catal. B: Environ. 267 (2020), 118717.
[21] N. Kishimoto, State of the art of UV/chlorine advanced oxidation processes: their mechanism, byproducts formation, process variation, and applications, J. Water Environ. Technol. 17 (2019) 302–335.
[22] X. Kong, Z. Wu, Z. Ren, K. Guo, S. Hou, Z. Hua, X. Li, J. Fang, Degradation of lipid regulators by the UV/chlorine process: radical mechanisms, chlorine oxide radical (ClO(*))-mediated transformation pathways and toxicity changes, Water Res. 137 (2018) 242–250.
[23] Q. Kong, X. Lei, X. Zhang, S. Cheng, C. Xu, B. Yang, X. Yang, The role of chlorine oxide radical (ClO(*)) in the degradation of polychoro-1,3-butadienes in UV/chlorine treatment: kinetics and mechanisms, Water Res. 183 (2020) 116056, https://doi.org/10.1016/j.watres.2020.116056.
[24] X. Kong, J. Jiang, J. Ma, Y. Yang, W. Liu, Y. Liu, Degradation of atrazine by UV/chlorine: efficiency, influencing factors, and products, Water Res. 90 (2016) 15–23.
[25] Z. Liu, Y.L. Lin, B. Xu, C.Y. Hu, T.Y. Zhang, T.C. Cao, Y. Pan, N.Y. Gao, Degradation of diiodoacetamide in water by UV/chlorination: kinetics, efficiency, influence factors and toxicity evaluation, Chemosphere 240 (2020), 124761.
[26] K. Guo, Z. Wu, C. Shang, B.o. Yao, S. Hou, X. Yang, W. Song, J. Fang, Radical chemistry and structural relationships of PPCP degradation by UV/chlorine treatment in simulated drinking water, Environ. Sci. Technol. 51 (18) (2017) 10431–10439.
[27] J. Xing, H. Wang, X. Cheng, X. Tang, X. Luo, J. Wang, T. Wang, G. Li, H. Liang, Application of low-dosage UV/chlorine pre-oxidation for mitigating ultrafiltration (UF) membrane fouling in natural surface water treatment, Chem. Eng. J. 344 (2018) 62–70.
[28] X. Lu, Y. Shao, N. Gao, J. Chen, H. Deng, W. Chu, N. An, F. Peng, Investigation of clofibric acid removal by UV/persulfate and UV/chlorine processes: kinetics and formation of disinfection byproducts during subsequent chlor(am)ination, Chem. Eng. J. 331 (2018) 364–371.
[29] J. Fang, Y. Fu, C. Shang, The roles of reactive species in micropollutant degradation in the UV/free chlorine system, Environ. Sci. Technol. 48 (3) (2014) 1859–1868.
[30] Y. Wang, M. Couet, L. Gutierrez, S. Allard, J.P. Croue, Impact of DOM source and character on the degradation of primidone by UV/chlorine: reaction kinetics and disinfection by-product formation, Water Res. 172 (2020), 115463.
[31] I. Carra, J. Fernandez Lozano, O. Autin, J.R. Bolton, P. Jarvis, Disinfection by-product formation during UV/Chlorine treatment of pesticides in a novel UV-LED reactor at 285 nm and the mitigation impact of GAC treatment, Sci. Total Environ. 712 (2020), 136413.
[32] M. Pan, Z. Wu, C. Tang, K. Guo, Y. Cao, J. Fang, Emerging investigators series: comparative study of naproxen degradation by the UV/chlorine and the UV/H2O2 advanced oxidation processes, Environ. Sci.: Water Res. Technol. 4 (2018) 1219–1230.
[33] J.R. Bolton, M.I. Stefan, P.-S. Shaw, K.R. Lykke, Determination of the quantum yields of the potassium ferrioxalate and potassium iodide–iodate actinometers and a method for the calibration of radiometer detectors, J. Photochem. Photobiol. A: Chem. 222 (2011) 166–169.
[34] Y. Chu, L. Xu, L. Gan, W. Qiao, J. Han, X. Mei, H. Guo, W. Li, C. Pei, H. Gong, X. Guo, Efficient destruction of emerging contaminants in water by UV/S(IV) process with natural reoxygenation: effect of pH on reactive species, Water Res. 198 (2021), 117143.
[35] K. Kutschera, H. Börnick, E. Worch, Photoinitiated oxidation of geosmin and 2-methylisoborneol by irradiation with 254 nm and 185 nm UV light, Water Res. 43 (8) (2009) 2224–2232.
[36] R. Yin, L.i. Ling, C. Shang, Wavelength-dependent chlorine photolysis and subsequent radical production using UV-LEDs as light sources, Water Res. 142 (2018) 452–458.
[37] K. Yin, Y. Deng, C. Liu, Q. He, Y. Wei, S. Chen, T. Liu, S. Luo, Kinetics, pathways and toxicity evaluation of neonicotinoid insecticides degradation via UV/chlorine process, Chem. Eng. J. 346 (2018) 298–306.
[38] F. Ghanbari, A. Yaghoot-Nezhad, S. Waclawek, K.A. Lin, J. Rodriguez-Chueca, F. Mehdipour, Comparative investigation of acetaminophen degradation in aqueous solution by UV/Chlorine and UV/H2O2 processes: kinetics and toxicity assessment, process feasibility and products identification, Chemosphere 285 (2021), 131455.
[39] Y. Pan, X. Li, K. Fu, Z. Gu, J. Shi, H. Deng, Overlooked role of secondary radicals in the degradation of beta-blockers and toxicity change in UV/chlorine process, Chem. Eng. J. 391 (2020), 123606.
[40] K. Guo, Z. Wu, S. Yan, B. Yao, W. Song, Z. Hua, X. Zhang, X. Kong, X. Li, J. Fang, Comparison of the UV/chlorine and UV/H2O2 processes in the degradation of PPCPs in simulated drinking water and wastewater: kinetics, radical mechanism and energy requirements, Water Res. 147 (2018) 184–194.
[41] U. von Gunten, Ozonation of drinking water: part II disinfection and by-product formation in presence of bromide, iodide or chlorine, Water Res. 37 (2003) 1469–1487.
[42] H.V. Lutze, N. Kerlin, T.C. Schmidt, Sulfate radical-based water treatment in presence of chloride: formation of chlorate, inter-conversion of sulfate radicals into hydroxyl radicals and influence of bicarbonate, Water Res. 72 (2015) 349–360.
[43] W. Yang, Y. Tang, L. Liu, X. Peng, Y. Zhong, Y. Chen, Y. Huang, Chemical behaviors and toxic effects of ametryn during the UV/chlorine process, Chemosphere 240 (2020), 124941.
[44] Z. Wu, K. Guo, J. Fang, X. Yang, H. Xiao, S. Hou, X. Kong, C. Shang, X. Yang, F. Meng, L. Chen, Factors affecting the roles of reactive species in the degradation of micropollutants by the UV/chlorine process, Water Res. 126 (2017) 351–360.
[45] Z. Hua, K. Guo, X. Kong, S. Lin, Z. Wu, L. Wang, H. Huang, J. Fang, PPCP degradation and DBP formation in the solar/free chlorine system: effects of pH and dissolved oxygen, Water Res. 150 (2019) 77–85.
[46] J. Liu, F. An, M. Li, L.u. Yang, J. Wan, S. Zhang, Efficient degradation of 2,4-Dichlorophenol on activation of peroxymonosulfate mediated by MnO2, Bull. Environ. Contam. Toxicol. 107 (2) (2021) 255–262.
[47] T. Li, Y. Jiang, X. An, H. Liu, C. Hu, J. Qu, Transformation of humic acid and halogenated byproduct formation in UV-chlorine processes, Water Res. 102 (2016) 421–427.
[48] S. Li, X. Ao, C. Li, Z. Lu, W. Cao, F. Wu, S. Liu, W. Sun, Insight into PPCP degradation by UV/NH2Cl and comparison with UV/NaClO: kinetics, reaction mechanism, and DBP formation, Water Res. 182 (2020), 115967.
[49] W.L. Wang, Q.Y. Wu, N. Huang, T. Wang, H.Y. Hu, Synergistic effect between UV and chlorine (UV/chlorine) on the degradation of carbamazepine: influence factors and radical species, Water Res. 98 (2016) 190–198.
[50] K. Yin, Q. He, C. Liu, Y. Deng, Y. Wei, S. Chen, T. Liu, S. Luo, Prednisolone degradation by UV/chlorine process: influence factors, transformation products and mechanism, Chemosphere 212 (2018) 56–66.
[51] R. Zabar, T. Komel, J. Fabjan, M.B. Kralj, P. Trebse, Photocatalytic degradation with immobilised TiO(2) of three selected neonicotinoid insecticides: imidacloprid, thiamethoxam and clothianidin, Chemosphere 89 (2012) 293–301.
[52] D. Guo, Y. Guo, Y. Huang, Y. Chen, X. Dong, H. Chen, S. Li, Preparation and electrochemical treatment application of Ti/Sb-SnO2-Eu&rGO electrode in the degradation of clothianidin wastewater, Chemosphere 265 (2021), 129126.
[53] J. Kuang, J. Huang, B. Wang, Q. Cao, S. Deng, G. Yu, Ozonation of trimethoprim in aqueous solution: identification of reaction products and their toxicity, Water Res. 47 (2013) 2863–2872.